




An FSS-based shared-aperture antenna for 5G/Wi-Fi communication and indoor 5G blind compensation

cambridge.org/mrf

Yu Lu Fan^{1,2} , Xian Qi Lin^{1,2} and Xinmi Yang^{1,2}

¹School of Electronic Science and Engineering, University of Electronic Science and Technology of China, Chengdu 611731, P. R. China and ²The Yangtze Delta Region Institute (Huzhou), University of Electronic Science and Technology of China, Huzhou 313001, P. R. China

Research Paper

Cite this article: Fan YL, Lin XQ, Yang X (2023). An FSS-based shared-aperture antenna for 5G/Wi-Fi communication and indoor 5G blind compensation. *International Journal of Microwave and Wireless Technologies* **15**, 1373–1381. <https://doi.org/10.1017/S1759078722001350>

Received: 3 July 2022
Revised: 25 October 2022
Accepted: 27 October 2022

Key words:

Blind compensation; frequency selective surface (FSS); indoor communication; shared aperture; Wi-Fi; 5G

Author for correspondence:

Xian Qi Lin, E-mail: xqlin@uestc.edu.cn

Abstract

In this paper, a frequency selective surface (FSS) based shared-aperture antenna is designed for 5G/Wi-Fi applications. The 5G and Wi-Fi channel are separated to achieve different polarizations and simultaneous work. The proposed antenna is of $\pm 45^\circ$ -polarization in the 5G N79 band and vertical polarization in the Wi-Fi 5.8 GHz band. The antenna is vertically stacked with the N79 band antenna located above the Wi-Fi band antenna. The N79 antenna is composed of FSS units with transmissive characteristics in the Wi-Fi band, and serves as an electromagnetically transparent surface to avoid blocking the Wi-Fi antenna. A prototype of our design is fabricated, assembled and tested, and measured results show that the prototype is able to cover the entire N79 band (4.1–5.2 GHz, 23.7%) and Wi-Fi 5.8 GHz band (5.73–5.89 GHz, 2.8%). Measured average gain is 8.2 and 7.8 dBi in the N79 and Wi-Fi band, respectively, and radiation efficiency is over 86 and 80%. The proposed design exhibits separated channels, tri-polarizations, high gain and compact size, which is sufficient for regular 5G/Wi-Fi applications. The antenna also achieves a relatively wide and highly consistent signal coverage in the two bands, making it suitable for 5G/Wi-Fi multi-function communication and indoor 5G blind compensation.

Introduction

The 5th Generation Mobile Communication Technology (5G) has significant advantages of high speed, low latency, and large capacity [1]. In view of these merits, uninterrupted network service that is not affected by network switching may be possible by combining the 5G core network with Wi-Fi technology. This means routers can become small base stations to provide 5G access, which can reduce coverage blind spots of indoor 5G signals and alleviate the problem of network congestion to a certain extent.

One challenge to realize the above vision is to connect Wi-Fi-enabled terminals to the 5G network, which can be solved by shared-aperture antennas. Compared to traditional multi-band antenna, shared-aperture antenna is of compact size and low profile on the basis of multi-function, and can better manage the problem of limited installation space [2–6]. In many shared-aperture antenna designs, frequency selective surface (FSS) is employed for isolation improvement and scattering suppression [6–14]. By inserting an FSS layer with filtering, isolating [7–11] or transmissive [6, 12–14] capabilities, cross-band interference, coupling or blocking effects can be alleviated. Another challenge to combine 5G with Wi-Fi service is to achieve consistent signal coverage in the two bands. Generally, base station signals are of $\pm 45^\circ$ -polarization and Wi-Fi signals from routers are vertically polarized. To ensure good reception for users, antennas with 5G/Wi-Fi functions should preferably be able to achieve $\pm 45^\circ$ - and vertical polarization in the 5G and Wi-Fi band, respectively, which means that the 5G and Wi-Fi channel need to be separated with each other. But separated channels can lead to differences in signal coverage and affect the signal conversion efficiency between the 5G and Wi-Fi channel, which needs to be avoided for indoor 5G blind compensation through Wi-Fi signal.

Existing designs of antennas with 5G/Wi-Fi function are insufficient [15–24]. A four-port MIMO antenna is designed and matched in 2.45/5 GHz Wi-Fi band and 3.2–6 GHz 5G band [15]. The antenna is of low profile, with 5G and Wi-Fi signal sharing the same channel and polarization. Another Vivaldi-shaped MIMO antenna is designed for 5G indoor access and dual-band Wi-Fi application [16]. The antenna achieves compact size through ground reuse, but also exhibits the disadvantages of shared channel and single polarization. A tri-band dual-polarized slot antenna is designed for Wi-Fi 2.45/5 GHz and 5G sub-6 GHz operation [17]. The design achieves low profile and dual polarizations through one single channel. In [18], a low-profile wideband 5G/Wi-Fi antenna is proposed, with shared channel and single polarization for 5G and Wi-Fi bands. In [19], a Wi-Fi/WiMAX/5G textile antenna is designed and resonates at multiple frequencies in 2.4–37 GHz with narrow bandwidths (BWs) and

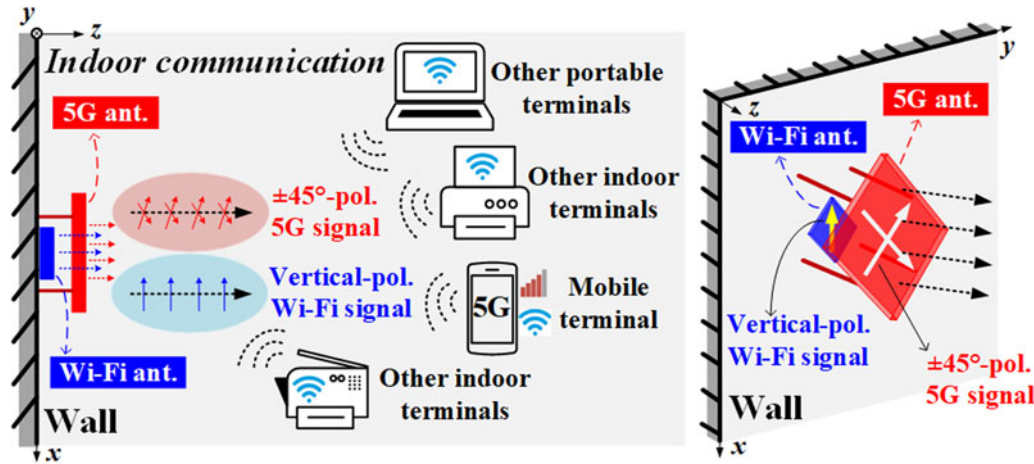


Fig. 1. Application scenarios of the proposed 5G/Wi-Fi antenna.

cluttered patterns at high frequencies, inapplicable for practical communication applications. In [20], a frequency tunable 5G/Wi-Fi antenna is proposed, which achieves tuning by connecting PIN diodes to different metamaterial units. But the antenna still has only one channel and polarization. In [21], an omnidirectional wideband dipole is designed for 5G/Wi-Fi/WiMAX applications, with only one channel covering the three bands. Another dipole-shaped single-channel antenna is designed with multiple resonances in 5G and Wi-Fi bands [22]. Both the dipole antennas in [21] and [22] are of single polarization. In [23], an ultra-wideband antenna with circular polarization is designed for 5G/WiFi-5/WiFi-6 multi-functions, but similar to [19], the antenna pattern becomes cluttered at high frequencies. All designs in [20–23] have not been fabricated and experimentally verified, and the results are only from simulations. In [24], a flexible transparent antenna for 5G N78/N79 band and 5 GHz Wi-Fi band is designed and fabricated. The antenna shows two impedance matching BWs of 3.5–3.578 and 4.79–5.09 GHz within one operating channel, and relatively low radiation efficiency of 33.4–57.3% due to the deformable structure of the antenna.

Notably, the above designs are essentially single-antenna designs with multiple bands or wide band covering the 5G and Wi-Fi bands, rather than integrated design that can support 5G and Wi-Fi functions simultaneously. To the authors best knowledge, the vast majority of existing 5G/Wi-Fi antennas do not possess the ability of signal conversion and blind compensation for the lack of separated channels, and there are few relevant studies on integration of 5G and Wi-Fi antennas. In this paper, on the basis of multi-band and multi-polarization, an FSS-based shared-aperture 5G/Wi-Fi antenna with separated channels is proposed. As shown in Fig. 1, the antenna is designed to be installed on the indoor wall with boresight parallel to the ground. The 5G and Wi-Fi channel are separated and can operate in different polarizations. The 5G antenna is of $\pm 45^\circ$ -polarization and meanwhile serves as an FSS layer for the vertically polarized Wi-Fi antenna. The proposed design can be employed as a 5G/Wi-Fi integrated terminal in application scenarios such as 5G/Wi-Fi multi-function communication and indoor 5G blind compensation.

Antenna design and working mechanism

As shown in Fig. 2, the proposed antenna consists of three F4B substrate layers ($\epsilon_r = 2.65$, $\tan \delta = 0.002$, $h_1 = h_3 = 1$ mm, $h_2 = 3$

mm). The uppermost layer and its upper and lower metal constitute the body of the N79 antenna. The middle layer and its upper metal constitute the body of the Wi-Fi antenna. The upper and lower metal of the lowermost layer are the metal ground and the feeding network, respectively. The middle and lowermost layer are bonded together, and the uppermost layer is fixed by four 3D-printing support pillars (photosensitive resin, $\epsilon_r = 2.87$, $\tan \delta = 0.015$) for better structural stability. Overall height of the antenna is $H = 16.5$ mm. The N79 antenna is composed of FSS units with electromagnetic transparency to avoid blocking the Wi-Fi antenna. The feeding network is designed beneath the ground plane. To achieve separated channels for 5G and Wi-Fi signals, the N79 antenna is fed by Port 1/2 through copper probes and the Wi-Fi antenna by Port 3 through metallized via.

Electromagnetic transparency of the N79 antenna

As shown in Fig. 2, the low-frequency N79 antenna is above the high-frequency Wi-Fi antenna. This structure layout makes better use of the vertical space, achieves the shared-aperture design and reduces the antenna profile. However, the upper N79 antenna with larger aperture exhibits coupling and blocking effects to the lower Wi-Fi antenna, so the N79 antenna needs to be specially designed to avoid damaging the normal operation of the Wi-Fi antenna.

Detailed structures and dimensions of the proposed 5G/Wi-Fi antenna are presented in Fig. 3. In this design, the N79 antenna operates not only as a radiator in the 5G band, but also as an FSS layer with electromagnetic transparency in the Wi-Fi band. As shown in Figs 3(a) and 3(b), the N79 antenna is actually deformed from a 4×4 array of the FSS unit shown in Fig. 3(c). Period of the FSS unit is $w = 6$ mm, which is much smaller than the free space wavelength at 5.8 GHz ($\lambda_{5.8} \approx 51.7$ mm). Therefore, special designs are needed for the FSS unit to be electromagnetically transparent in the Wi-Fi band.

Ref. A, B, C and D in Fig. 4(a) show the evolution process of the proposed FSS unit. Four FSS units (Ref. A–D) are simulated in Ansys HFSS, and the simulation model is shown in Fig. 4(b). Due to the structural symmetry of the FSS units, responses under two orthogonal port modes (Modes 1 and 2) are consistent. And according to basic electromagnetic theory, any polarization can be decomposed into two orthogonal components. Therefore, response of the FSS units under arbitrary polarization can be

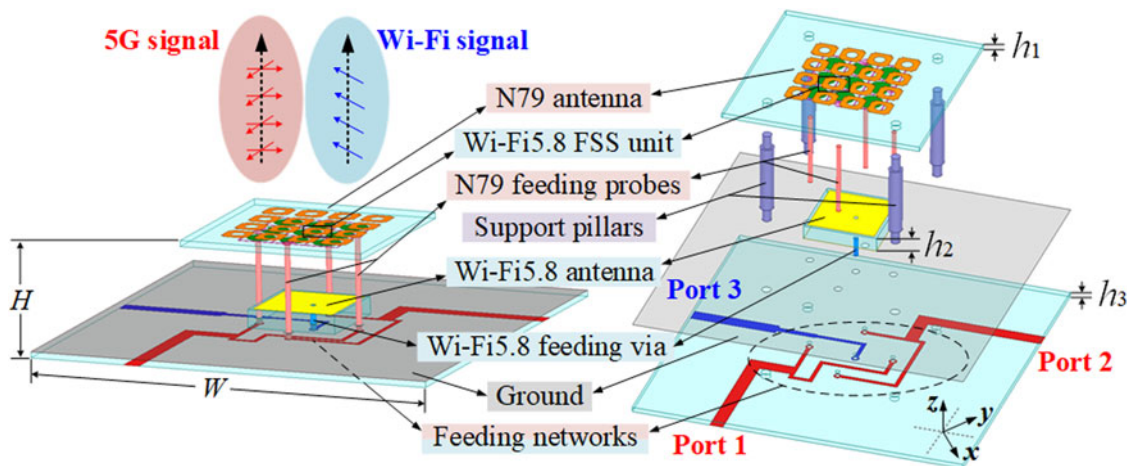


Fig. 2. Overall structure of the proposed 5G/Wi-Fi antenna.

revealed by analyzing the response under Mode 1 or 2. Simulated responses of different FSS units under Mode 1 are compared in Fig. 4(c). Ref. A is of basic cross grid structure with low-stop features at 5.8 GHz. Based on Ref. A, fan-shaped patches are added in Ref. B, and the resonance moves slightly towards 5.8 GHz. Meanwhile, a cross-shaped patch is also added in Ref. C, which exhibits similar performance as Ref. B, but neither is enough to resonate in the Wi-Fi band. Combine the structure of Ref. B and C yields Ref. D. With reasonable tuning of structural dimensions, Ref. D exhibits much better responses than Ref. B and C, as shown in Fig. 4(c). Therefore, unit Ref. D is a qualified candidate for the FSS unit in this design.

As shown in Figs 5(a) and 5(b), corresponding to FSS units Ref. A-D, different N79 antennas (Ant. A-D) are simulated and compared as well, with results shown in Fig. 5(c). The cross grid of the FSS unit constitutes a closed mesh structure, which is the main radiation part of the N79 antenna. Patch arrays

formed by the cross- and fan-shaped patches serve as the parasitic part of the mesh structure and improve the matching of the N79 antenna. The coupling structure shown in Fig. 3(d) is designed at the midpoint of each side of the closed mesh structure, and is further connected to the feeding network through a copper probe, so as to realize the excitation of the N79 antenna.

Notably, although Ref. D exhibits satisfying performance at 5.8 GHz, frequency response of Ant. D in the N79 band is not ideal, as shown in Fig. 5(c). Therefore, structure of Ref. D is further modified by etching a circular hole on the cross-shaped patch to improve the impedance matching of Ant. D. Finally, structure of the proposed FSS unit and the N79 antenna are decided. Simulation results of the proposed FSS unit and the N79 antenna are added to Figs 4(b) and 5(c), respectively, and the former shows good electromagnetic transparency in the Wi-Fi band while frequency response of the latter is also satisfying.

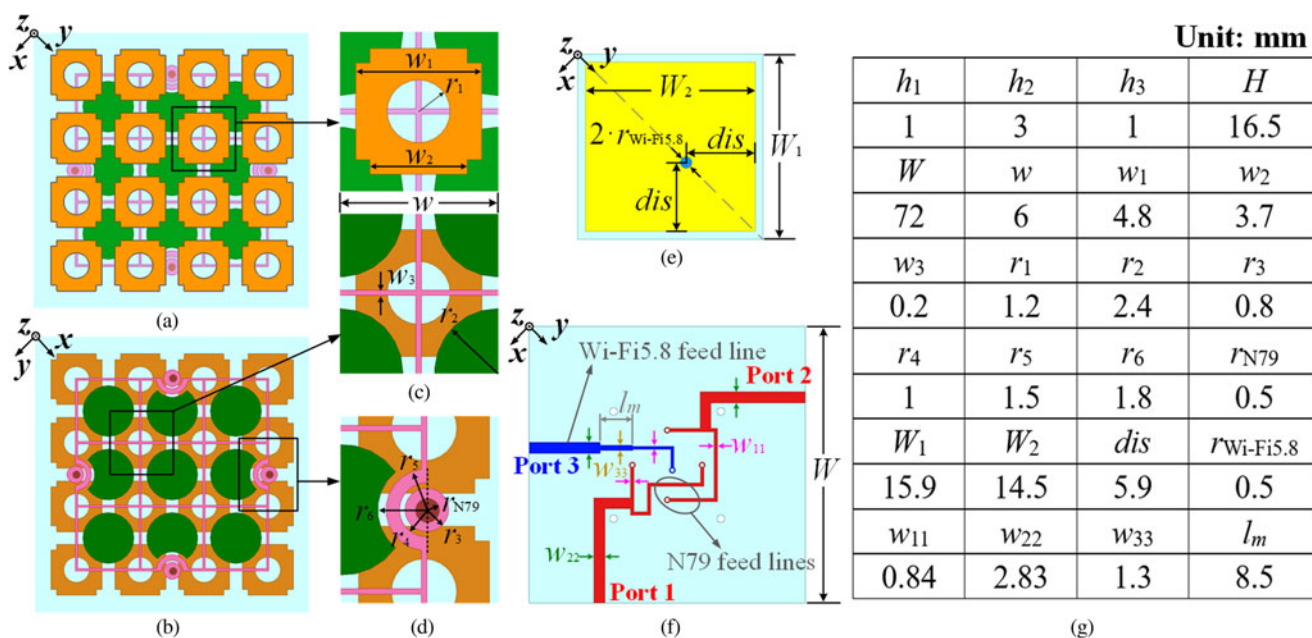
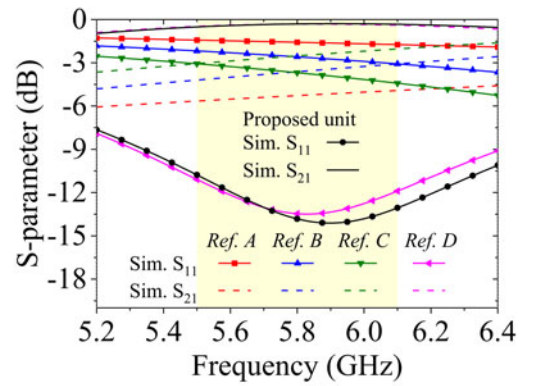
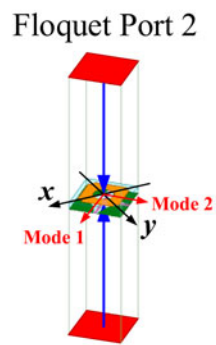


Fig. 3. (a) Top and (b) bottom view of the N79 antenna. (c) FSS unit. (d) Coupling structure of the N79 antenna. (e) Top view of the Wi-Fi antenna. (f) Feeding network. (g) Dimensions.

Wi-Fi5.8 FSS unit	Ref. A	Ref. B	Ref. C	Ref. D	Proposed unit
Top view					
Bottom view					

(a)



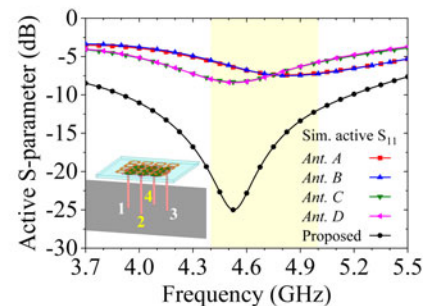
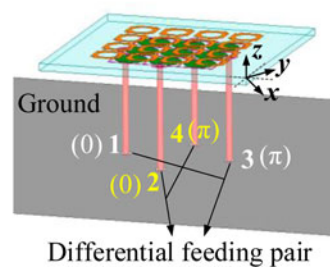
(c)

Fig. 4. (a) Evolution process of the FSS unit. (b) Simulation model and port modes of the FSS unit. (c) Frequency response of different FSS units (under Mode 1).

(b)

N79 antenna	Ant. A	Ant. B	Ant. C	Ant. D	Proposed antenna
Top view					
Bottom view					

(a)



(c)

Fig. 5. (a) Different N79 antennas. (b) Simulation model of the N79 antenna. (c) Frequency responses of different N79 antennas.

(b)

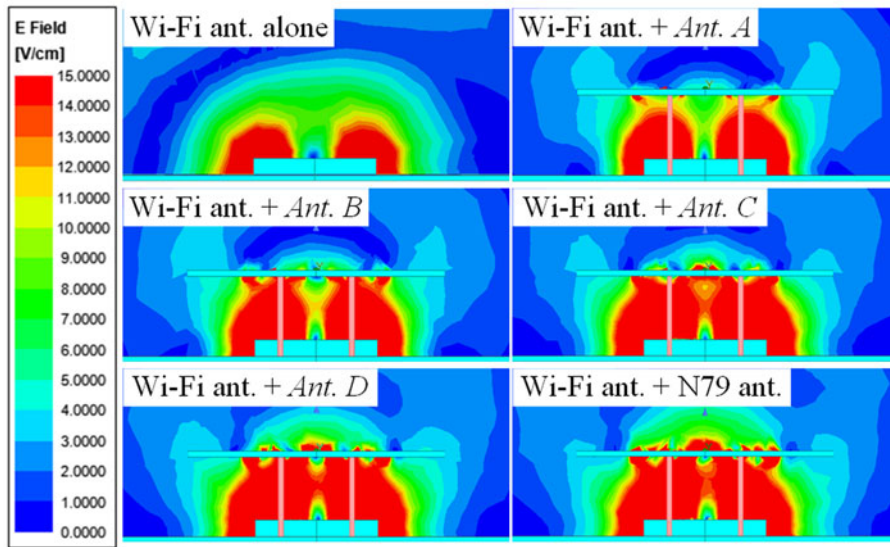


Fig. 6. E-field distribution of the Wi-Fi antenna under different situations.

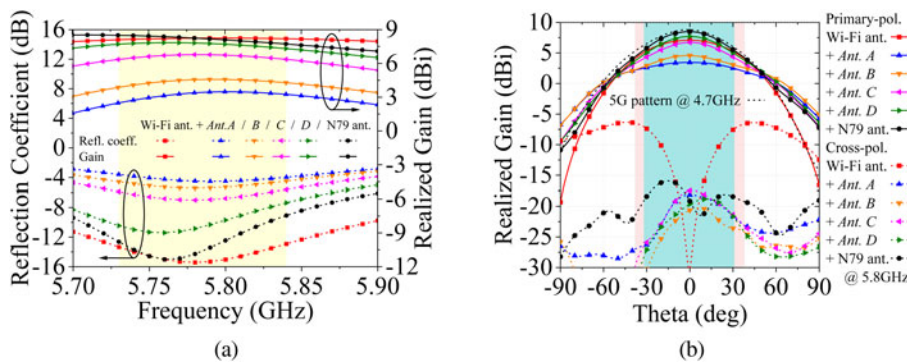


Fig. 7. (a) Frequency response, antenna gain and (b) radiation pattern of the Wi-Fi antenna under different situations.

Working of the Wi-Fi antenna

The Wi-Fi antenna is a single-fed rectangular patch, as demonstrated in Fig. 3(e). Due to space limitations, the substrate is of nearly equivalent size as the patch for assembly simplicity. Feed point of the Wi-Fi antenna is located on the diagonal of the patch with a certain distance from the center, thus the antenna polarization is along the diagonal.

To further verify the normal operation of the Wi-Fi antenna, antenna performance at 5.8 GHz under different situations (Wi-Fi5.8 ant. alone, Wi-Fi5.8 ant. with *Ant. A/B/C/D/proposed*

N79 ant.) are simulated and compared. Figure 6 compares the spatial E-field distribution. It can be observed that *Ant. A, B* and *C* exhibit obvious blocking effect on the Wi-Fi antenna. Radiation of the Wi-Fi antenna can hardly pass through with weakened E-field in the upper space. However, *Ant. D* and the proposed *N79* antenna can effectively reduce the blocking effect and restore the E-field in the upper space. As shown in Fig. 7, the presence of *Ant. A, B* or *C* deteriorates the matching and gain of the Wi-Fi antenna, while *Ant. D* and the proposed *N79* antenna lead to better matching (Reflection coefficient < -10 dB) and antenna gain (Realized gain > 7.5 dBi).

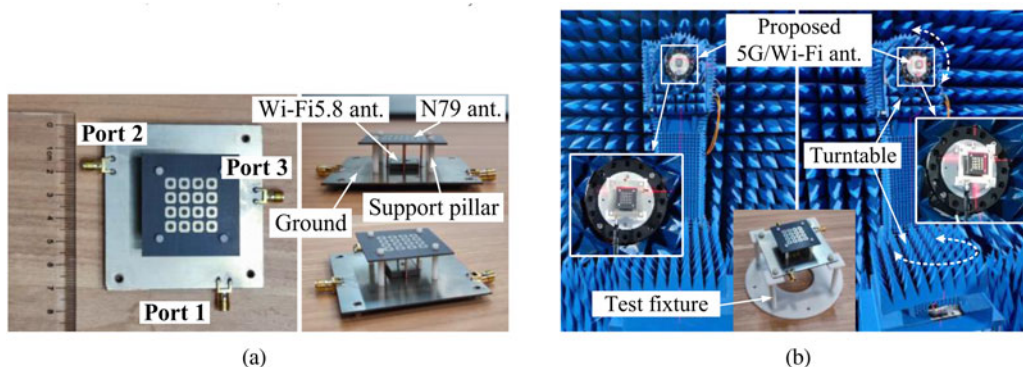


Fig. 8. (a) Overall assembly and (b) test setup of the prototype.

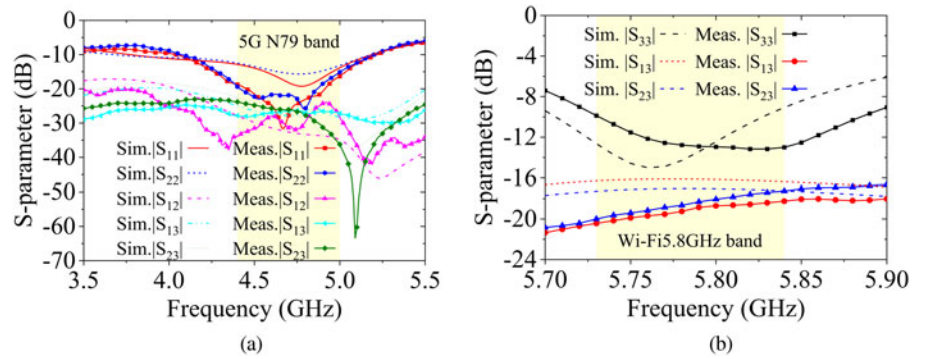


Fig. 9. S-parameters of the prototype in the (a) N79 and (b) Wi-Fi band.

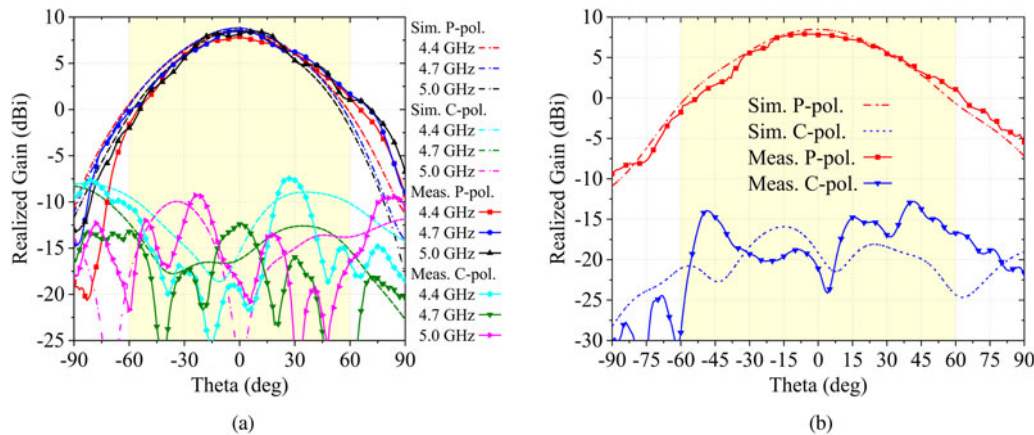


Fig. 10. Radiation patterns of the prototype at (a) 4.4, 4.7, 5.0 and (b) 5.8GHz.

Notably, the aperture of the N79 antenna also plays a role in guiding and constraining the radiation field of the Wi-Fi antenna, which contributes to improved directivity and enhanced gain of the Wi-Fi antenna. As shown in Fig. 7(b), the pink and blue areas are the half power beam widths (HPBW's) of the Wi-Fi antenna with and without the N79 antenna, respectively. It can be observed that the latter exhibits better directivity, narrower HPBW and higher gain. Also, the constraining effect of the N79 antenna leads to similar pattern features for the proposed 5G/Wi-Fi antenna in the two operating bands, so as to achieve relatively consistent beam coverages.

Antenna feeding mechanism

As demonstrated in Fig. 2, the feeding network of the proposed antenna is designed beneath the metal ground to minimize the interference of the microstrip lines on antenna radiation, and meanwhile improve the space utilization. The feeding network includes two differential feeding lines for the N79 antenna and one 50-to-100-Ω feeding line for the Wi-Fi antenna, as presented in Fig. 3(f).

For the N79 antenna, Port 1 and 2 correspond to the +45°- and -45°-polarization, respectively. Each differential feeding line includes a T-junction and two branches with 180° phase

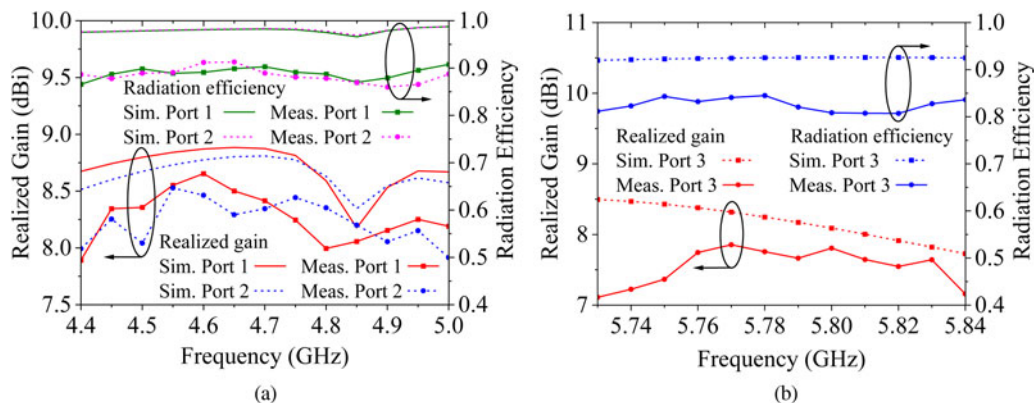


Fig. 11. Antenna gain and radiation efficiency in the (a) N79 and (b) Wi-Fi band.

Table 1. Comparison of different antennas with 5G/Wi-Fi functions

Application	BW (GHz) ($ S_{11} < -10$ dB)	Channel	Polarization	HPBW	Gain (dBi)	Radiation efficiency	Antenna size
[15] Wi-Fi2.45/5.0 5G sub-6	2.7–3.5 (25.8%) 4.5–6.5 (36.4%)	Shared	Single linear	–	–	34.1–66.2% 39.6%/60.7%	$27.7 \times 27.7 \times 1.2$ mm ³ $0.25 \times 0.25 \times 0.011$ mm ^{2,7}
[16] 5G sub-6 Wi-Fi2.45/5.5	2.4–3 (22.2%) 5.1–5.5 (7.5%)	Shared	Single linear	–	3–6 9–10.2	60–70%	$137 \times 137 \times 1.2$ mm ³ $1.1 \times 1.1 \times 0.01$ mm ^{2,4}
[17] Wi-Fi2.45 5G sub-6 Wi-Fi5.0	2.4–2.51 (4%) 3.29–3.6 (8%) 4.8–5.05 (4%)	Shared	Dual linear	60° 50° 65°	5 6 6.5	80% 82% 90%	$85 \times 85 \times 6.8$ mm ³ $0.68 \times 0.68 \times 0.054$ mm ^{2,4}
[18] 5G sub-6 Wi-Fi5.8	4.96–5.94 (18.1%)	Shared	Single linear	25°–40°	8.4– 10.9	58–78%	$61.8 \times 61.8 \times 4.2$ mm ³ $1.03 \times 1.03 \times 0.07$ mm ^{2,5,0}
[19] Wi-Fi2.4 WiMAX7.8 5G	2.36 (3.2%) 7.8 (1.8%) 22.86/25.81 (6.8%), 29.43 (7.2%), 32–37 (14.5%)	Shared	Single linear	74° 41.8° –	7.55 5.85 –	98% 93% 88–95%	$108 \times 80 \times 1.5$ mm ³ $0.85 \times 0.63 \times 0.012$ mm ^{2,4}
[21] ^a 5G Wi-Fi WiMAX	3–6.26 (70.4%)	Shared	Single linear	Omni directional	2.4–3.4	93.2%	$36 \times 31 \times 0.79$ mm ³ $0.36 \times 0.31 \times 0.008$ mm ^{2,3,0}
[22] ^a IoT/5G/Wi-Fi	4.5 (9.1%), 5.8 (11.3%), 7 (11%), 8.7 (6.8%)	Shared	Single linear	Omni directional	4.35	–	$40 \times 15 \times 1.6$ mm ³ $0.6 \times 0.23 \times 0.02$ mm ^{2,3,4,5}
[23] ^a 5G Wi-Fi	3.7–4.2 (12.7%), 4.4–5.0 (12.8%), 24.25–29.5 (19.5%) 5.15–5.85 (12.7%), 5.93–7.13 (18.4%)	Shared	Single circular	Omni directional	1.25– 8.7	64–92%	$34 \times 32 \times 1.6$ mm ³ $0.42 \times 0.4 \times 0.02$ mm ^{2,3,7}
[24] 5G N78/N79 Wi-Fi5.0	3.5–3.578 (2.2%), 4.79–5.09 (6.1%)	Shared	Single linear	64°–70°	2.5–4	33.4–57.3%	–
This work Wi-Fi5.8	4.1–5.2 (23.7%) 5.73–5.89 (2.8%)	Separated	±45° linear Vertical	61°–70° 68°	7.9–8.9 7.1–7.8	86–92% 80–85%	$72 \times 72 \times 16.5$ mm ³ $0.98 \times 0.98 \times 0.23$ mm ^{2,3,4,1}

^aDesigns in Ref. [21–23] are not fabricated and experimentally verified, and the presented results are only from simulations.

difference. The end of each branch is connected with a copper probe, which is further connected to the coupling structure shown in Fig. 3(d). By feeding Port 1 (or 2), differential excitation can be generated on the opposite sides of the N79 antenna, thereby achieving linear polarization.

For the Wi-Fi antenna, Port 3 corresponds to the vertical polarization. As shown in Fig. 3(f), the 50-to-100- Ω feeding line consists of a $\lambda/4$ impedance matching branch, which matches the high impedance of the Wi-Fi antenna to the 50 Ω port. The end of the feeding line is connected to the antenna patch through a metalized via to excite the Wi-Fi antenna.

Experimental results and discussion

A prototype of the designed antenna is fabricated, assembled and tested, as shown in Fig. 8. Overall dimension of the prototype is $72 \times 72 \times 16.5 \text{ mm}^3$ ($0.98 \times 0.98 \times 0.23\lambda^3$ @ 4.1 GHz), and the radiation aperture of the N79 and Wi-Fi antenna are $23 \times 23 \times 16.5 \text{ mm}^3$ ($0.31 \times 0.31 \times 0.23\lambda_{4.1}^3$) and $14.5 \times 14.5 \times 4 \text{ mm}^3$ ($0.28 \times 0.28 \times 0.077\lambda_{5.8}^3$), respectively. The prototype is mounted on a 3D-printing test fixture (photosensitive resin, $\epsilon_r = 2.87$, $\tan \delta = 0.015$) and tested in the microwave anechoic chamber.

Measured frequency responses in the N79 and Wi-Fi 5.8 GHz band are shown in Fig. 9. Reflection coefficient of Port 1/2 is below -10 dB in the 5G band (4.1–5.2 GHz, 23.7%), with isolation over 24 dB. Reflection coefficient of Port 3 is below -10 dB in the Wi-Fi band (5.73–5.89 GHz, 2.8%), with a slight frequency offset due to assembly errors introduced by the conductive glue used to bond the middle and lowermost layer. Figure 9 also shows that, the isolation between the 5G channel (Port 1 and 2) and the Wi-Fi channel (Port 3), i.e. $|S_{13}|$ and $|S_{23}|$, are no less than 23 and 16 dB in the N79 and Wi-Fi band, respectively, which indicates good port isolation and low mutual coupling between the N79 antenna and the Wi-Fi antenna in the two bands.

Figures 10(a) and 10(b) present the E-plane radiation patterns at 4.4/4.7/5.0 GHz when Port 1 is excited and 5.8 GHz when Port 3 is excited, respectively. HPBW in the N79 and Wi-Fi band are 61° – 77° ($-37^\circ \sim 40^\circ$ @4.4 GHz, $-34^\circ \sim 40^\circ$ @4.7 GHz, $-31^\circ \sim 30^\circ$ @5.0 GHz) and 70° ($-34^\circ \sim 36^\circ$ @5.8 GHz), with boresight cross-polarization below -20 and -27 dB, respectively. 3-dB beam coverage of the prototype in the 5G and Wi-Fi band is highly consistent, which is beneficial for high-efficiency signal conversion in indoor signal blind compensation.

Antenna gain and radiation efficiency is shown in Fig. 11. Average gain of the prototype in the N79 and Wi-Fi band are 8.2 and 7.8 dBi, respectively, and radiation efficiency is over 86 and 80%.

Comparison is made between some existing designs of 5G/Wi-Fi antennas and this work, as shown in Table 1. Our design is able to cover the entire 5G N79 and Wi-Fi 5.8 GHz band with separated channels, tri-polarizations, consistent signal coverage, high gain and compact size, sufficient for 5G/Wi-Fi communication and indoor 5G blind compensation.

Conclusion

This paper presents an FSS-based shared-aperture antenna for 5G/Wi-Fi communication and indoor 5G blind compensation. The $\pm 45^\circ$ -polarized 5G antenna operates in the N79 band with electromagnetic transparency to avoid blocking the vertically polarized Wi-Fi 5.8 GHz antenna. The proposed design operates in 4.1–5.2 GHz (5G, 23.7%) and 5.73–5.89 GHz (Wi-Fi, 2.8%) with antenna average gain of 8.2 and 7.8 dBi and radiation

efficiency of 86–92% and 80–85%, respectively. 3-dB beam coverage of the antenna is relatively wide and highly consistent (61° – 70° in the N79 band and 70° at 5.8 GHz), which makes the proposed design a promising candidate for 5G/Wi-Fi communication and high-efficiency signal conversion in indoor 5G blind compensation.

Acknowledgements. This work was supported in part by the National Natural Science Foundation of China under Grant No. 61871280.

Conflict of interest. The authors report no conflict of interest.

References

1. Wang Z, Ning Y and Dong Y (2022) Hybrid metamaterial-TL-based, low-profile, dual-polarized omnidirectional antenna for 5G indoor application. *IEEE Transactions on Antennas and Propagation* **70**, 2561–2570.
2. Han Y, Gong S, Wang J, Li Y, Fan Y, Zhang J and Qu S (2020) Shared-aperture antennas based on even- and odd-mode spoof surface plasmon polaritons. *IEEE Transactions on Antennas and Propagation* **68**, 3254–3258.
3. Liu ZG, Yin RJ, Ying ZN, Lu WB and Tseng KC (2021) Dual-band and shared-aperture Fabry–Perot cavity antenna. *IEEE Antennas and Wireless Propagation Letters* **20**, 1686–1690.
4. Ji S, Dong Y, Wen S and Fan Y (2021) C/X dual-band circularly polarized shared-aperture antenna. *IEEE Antennas and Wireless Propagation Letters* **20**, 2334–2338.
5. Bae JH and Yoon YJ (2021) 5G dual (S-/Ka-) band antenna using thick patch containing slotted cavity array. *IEEE Antennas and Wireless Propagation Letters* **20**, 1008–1012.
6. Yang SJ and Zhang XY (2022) Frequency selective surface-based dual-band dual-polarized high-gain antenna. *IEEE Transactions on Antennas and Propagation* **70**, 1663–1671.
7. Zhu Y, Chen Y and Yang S (2019) Decoupling and low-profile design of dual-band dual-polarized base station antennas using frequency-selective surface. *IEEE Transactions on Antennas and Propagation* **67**, 5272–5281.
8. Zhu Y, Chen Y and Yang S (2021) Cross-band mutual coupling reduction in dual-band base-station antennas with a novel grid frequency selective surface. *IEEE Transactions on Antennas and Propagation* **69**, 8991–8996.
9. He D, Chen Y and Yang S (2022) A low-profile triple-band shared-aperture antenna array for 5G base station applications. *IEEE Transactions on Antennas and Propagation* **70**, 2732–2739.
10. Zhou C, Yuan S, Li H, Wang B and Wong H (2021) Dual-band shared-aperture antenna with bifunctional metasurface. *IEEE Antennas and Wireless Propagation Letters* **2**, 2013–2017.
11. Abdollahvand M, Forooghi K, Encinar JA, Atlasbaf Z and Martinez-de-Rioja E (2020) A 20/30 GHz reflectarray backed by FSS for shared aperture Ku/Ka-band satellite communication antennas. *IEEE Antennas and Wireless Propagation Letters* **19**, 566–570.
12. Zhou GN, Sun BH, Liang QY, Wu ST, Yang YH and Cai YM (2021) Triband dual-polarized shared-aperture antenna for 2G/3G/4G/5G base station applications. *IEEE Transactions on Antennas and Propagation* **69**, 97–108.
13. He D, Yu Q, Chen Y and Yang S (2021) Dual-band shared-aperture base station antenna array with electromagnetic transparent antenna elements. *IEEE Transactions on Antennas and Propagation* **69**, 5596–5606.
14. Mei P, Lin XQ, Pedersen GF and Zhang S (2021) Design of a triple-band shared-aperture antenna with high figures of merit. *IEEE Transactions on Antennas and Propagation* **69**, 8884–8889.
15. Haskou A, Pesin A, Le Naour JY and Louzir A (2018) Four-port, broadband, compact antenna for 5G indoor access and content distribution over Wi-Fi. *Int. Conf. High Performance Computing & Simulation (HPCCS)*, Orleans, France.
16. Haskou A, Pesin A, Naour JL and Louzir A (2019) Compact, integrated, four-sector, antenna for sub-6GHz 5G indoor access and content distribution over Wi-Fi. *49th European Microwave Conf. (EuMC)*, Paris, France.
17. Cui Y, Wang X, Shen G and Li R (2020) A triband SIW cavity-backed differentially fed dual-polarized slot antenna for Wi-Fi/5G applications. *IEEE Transactions on Antennas and Propagation* **68**, 8209–8214.

18. Nie NS, Yang XS, Chen ZN and Wang BZ (2020) A low-profile wide-band hybrid metasurface antenna array for 5G and Wi-Fi systems. *IEEE Transactions on Antennas and Propagation* **68**, 665–671.
19. Bhaladar H, Gowre SK, Mathpati MM, Ustad MS, Jadhav AA and Mankal P (2021) Multiband microstrip textile antenna for Wi-Fi/WiMAX/5G communication. *IEEE 4th Int. Conf. Computing, Power and Commun. Tech. (GUCON)*, Beijing, China.
20. Orugu R, Nesasudha M and Janapala DK (2021) A frequency tunable hexagon shaped antenna for 5.8GHz-Wi-Fi and sub 6 – 5G Mobile IoT applications. *Int. Conf. Computer Commun. and Informatics (ICCCI)*, Nagoya, Japan.
21. Paul LC, Jim MTR, Rani T, Samsuzzaman M, Rahman MS and Azim R (2022) An omni-directional rectangular patch antenna for 5G/WiFi/WiMAX applications. *Int. Conf. Innov. Sci., Eng. Technol. (ICISET)*, Chittagong, Bangladesh.
22. Ka'bi AA (2022) Proposed antenna design for IoT and 5G-WiFi applications. *IEEE World AI IoT Congress (AIoT)*, Seattle, WA, USA.
23. Hyasat YMA, Faouri YS and Abualnadi D (2022) Multi-function dual UWB patch antenna for modern communications. *Int. Telecommun. Conf. (ITC-Egypt)*, Alexandria, Egypt.
24. Yu BY, Wang ZH, Ju L, Zhang C, Liu ZG, Tao L and Lu WB (2022) Flexible and wearable hybrid RF and solar energy harvesting system. *IEEE Transactions on Antennas and Propagation* **70**, 2223–2233.



Yu Lu Fan (student member, IEEE (Institute of Electrical and Electronics Engineers)) was born in Luoyang, Henan, China, in 1997. She earned B.S. in electronic engineering from the University of Electronic Science and Technology of China (UESTC), Chengdu, China, in 2019, where she is currently pursuing Ph.D. at the School of Electronic Science and Engineering. Her current research interests include millimeter-wave and terahertz technologies, metamaterials, and transmit-/reflect-arrays.



Xian Qi Lin (senior member, IEEE) was born in Taizhou, Zhejiang, China, in 1980. He earned B.S. in electronic engineering from the University of Electronic Science and Technology of China (UESTC), Chengdu, China, in 2003, and Ph.D. in electromagnetic and microwave technology from Southeast University, Nanjing, China, in 2008. In 2009, he joined the Department of Microwave Engineering, UESTC, where he was an associate professor and a doctoral supervisor in 2011. From 2011 to 2012, he was a post-doctoral researcher in the Department of Electromagnetic Engineering, KTH Royal Institute of Technology, Stockholm, Sweden. Currently he is a full professor with UESTC. He has authored over 40 scientific journal articles and 20 conference papers. He holds over 10 patents. His current research interests include microwave/millimeter-wave circuits, metamaterials, and antennas.



Xin Mi Yang was born in Suzhou, Jiangsu Province, China, in March 1982. He earned B.S. and Ph.D. from Southeast University, Nanjing, China, in 2005 and 2010, respectively, both in the School of Information Science and Engineering. In November 2010, he joined the School of Electronics and Information Engineering, Soochow University, Suzhou, China, and has been an associate professor since July 2014. Since 2021, he has been with the Yangtze Delta Region Institute (Huzhou) & School of Electronic Engineering, University of Electronic Science and Technology of China as an associate research fellow. He has authored and co-authored more than 40 technical journal articles. He co-edited the book *Metamaterials – Beyond Crystals, Noncrystals, and Quasicrystals* (CRC Press, June 2016) and is the author of two book chapters. His current research interests include metamaterials, metasurfaces, LTCC technology and their applications on antennas and microwave engineering.